

## RESEARCH ARTICLE

# Tead2 expression levels control the subcellular distribution of Yap and Taz, zyxin expression and epithelial–mesenchymal transition

Maren Diepenbruck<sup>1,\*</sup>, Lorenz Waldmeier<sup>1,\*</sup>, Robert Ivanek<sup>1</sup>, Philipp Berninger<sup>2</sup>, Phil Arnold<sup>2</sup>, Erik van Nimwegen<sup>2</sup> and Gerhard Christofori<sup>1,‡</sup>

**ABSTRACT**

The cellular changes during an epithelial–mesenchymal transition (EMT) largely rely on global changes in gene expression orchestrated by transcription factors. Tead transcription factors and their transcriptional co-activators Yap and Taz have been previously implicated in promoting an EMT; however, their direct transcriptional target genes and their functional role during EMT have remained elusive. We have uncovered a previously unanticipated role of the transcription factor Tead2 during EMT. During EMT in mammary gland epithelial cells and breast cancer cells, levels of Tead2 increase in the nucleus of cells, thereby directing a predominant nuclear localization of its co-factors Yap and Taz via the formation of Tead2–Yap–Taz complexes. Genome-wide chromatin immunoprecipitation and next generation sequencing in combination with gene expression profiling revealed the transcriptional targets of Tead2 during EMT. Among these, zyxin contributes to the migratory and invasive phenotype evoked by Tead2. The results demonstrate that Tead transcription factors are crucial regulators of the cellular distribution of Yap and Taz, and together they control the expression of genes critical for EMT and metastasis.

**KEY WORDS:** Breast cancer, EMT, metastasis, Taz, Tead, Yap, Zyxin

**INTRODUCTION**

Epithelial–mesenchymal transition (EMT) is a cell-biological program that is required at various stages of embryonic development. Activation of EMT in epithelial cells induces a loss of cell–cell adhesions and apical–basal polarity, and promotes trans-differentiation into a mesenchymal state, which is characterized by a migratory and invasive phenotype (Kalluri and Weinberg, 2009; Nieto, 2011). During solid tumor progression, a reactivation of some of these features in epithelial tumor cells (oncogenic EMT) is regarded as one of the mechanisms that can facilitate metastatic spread (Chaffer and Weinberg, 2011; Thiery et al., 2009). Oncogenic EMT not only provides tumor cells with invasive properties that permit dissemination from the primary

tumor, but also results in the acquisition of stem-cell-like traits, which has implications for cancer therapy and might also be important for colonization at distant organs (Chaffer and Weinberg, 2011; Magee et al., 2012; Polyak and Weinberg, 2009; Scheel and Weinberg, 2012). Among the many genes and signaling pathways active during EMT, transcription factors are the master coordinators of the EMT program (Acloque et al., 2009; Moreno-Bueno et al., 2008; Nieto, 2011).

The Hippo tumor suppressor signaling pathway plays a critical role in restricting organ size by antagonizing the oncogenic transcriptional co-activators Yap and Taz (Hong and Guan, 2012; Zhao et al., 2011). A complex network of cell adhesion and signaling molecules, including the tumor suppressor neurofibromin-2/Merlin, regulates the Hippo kinase cascade, leading from the protein kinases Mst1 and Mst2 via the protein kinases Lats1 and Lats2 to the transcriptional co-factors Yap and Taz. When the Hippo pathway is active, Yap and Taz are phosphorylated by Lats1 and Lats2, and phosphorylated Yap and Taz are retained in the cytoplasm. In the absence of activated Hippo signaling, unphosphorylated Yap and Taz are imported into the nucleus where they, together with Tead DNA-binding transcription factors, activate the expression of proliferative and anti-apoptotic genes.

In mammals, Tead transcription factors comprise a family of four members (Tead1–Tead4). They are ubiquitously expressed (Jacquemin et al., 1996; Kaneko and DePamphilis, 1998) and exert partially redundant roles in regulating the development of various embryonic tissues, including neural crest, whose formation depends on EMT (Thiery et al., 2009), notochord and trophoblast (Milewski et al., 2004; Sawada et al., 2008; Sawada et al., 2005; Yagi et al., 2007). Transcriptional activity of the DNA-binding Teads requires their physical association with the transcriptional co-activators Yap or Taz (Mahoney et al., 2005; Vassilev et al., 2001). Upon Yap- or Taz-mediated activation, Teads can exert multiple functions. For example, they control proliferation in epithelial cells and fibroblasts (Ota and Sasaki, 2008; Zhang et al., 2009; Zhao et al., 2008b). Moreover, Yap and Taz are sufficient to induce EMT of MCF10A human breast epithelial cells in a Tead-dependent manner (Lei et al., 2008; Zhang et al., 2009; Zhao et al., 2008b), and the nuclear accumulation of Yap and Taz in Eph4 murine mammary epithelial cells is required for these cells to undergo TGFβ-induced EMT (Varelas et al., 2010b). Finally, elevated levels of Yap trigger increased tumor growth and a pro-metastatic phenotype through binding to Tead in breast cancer and melanoma cells (Lamar et al., 2012). Even though these studies clearly demonstrate a crucial role for Teads, Yap and Taz in mediating EMT induction and cancer progression, the mechanisms involved in the regulation of Tead transcriptional

<sup>1</sup>Department of Biomedicine, University of Basel, 4058 Basel, Switzerland.

<sup>2</sup>Biozentrum, University of Basel, and Swiss Institute of Bioinformatics, 4056 Basel, Switzerland.

\*These authors contributed equally to this work

<sup>‡</sup>Author for correspondence (Gerhard.christofori@unibas.ch)

This is an Open Access article distributed under the terms of the Creative Commons Attribution License (<http://creativecommons.org/licenses/by/3.0>), which permits unrestricted use, distribution and reproduction in any medium provided that the original work is properly attributed.

activity and the direct target genes during an EMT remain to be identified.

To delineate the mechanisms underlying the transcriptional activities of Teads and to identify their transcriptional target genes during EMT, we have utilized cellular model systems of EMT in non-transformed murine mammary gland epithelial cells and in murine breast cancer cells. We report that the expression of Tead family members is upregulated during EMT, concomitant with an overall increase in Tead transcriptional activity. We demonstrate that elevated levels of Tead2 lead to increased nuclear localization of Yap and Taz, where they form a complex with Tead2. As a result, increased Tead2 transcriptional activity provokes the induction of EMT and a malignant tumor phenotype. Conversely, knockdown of Teads in cells undergoing an EMT prevents efficient subcellular redistribution of Yap and Taz and blocks EMT. Genome-wide chromatin immunoprecipitation and next generation sequencing (ChIP-Seq) in combination with gene expression profiling identified several EMT-relevant genes as direct transcriptional targets of Tead2 during EMT. Among these, the gene encoding zyxin, a component of focal adhesions and an actin cytoskeleton remodeling protein, is required for EMT-related migration and invasion.

## RESULTS

### Formation of a nuclear Tead2–Yap–Taz complex and its transcriptional activity during EMT

To identify crucial genes underlying the multiple stages of an EMT, we induced EMT in the untransformed normal murine mammary gland cell line NMuMG (Maeda et al., 2005) by treatment with TGF $\beta$  for 0, 1, 4, 7, 10 and 20 days (data not shown). During this time course, the cells underwent progressive EMT and acquired a complete mesenchymal morphology (Lehembre et al., 2008). Motif Activity Response Analysis (MARA) (Suzuki et al., 2009) of gene expression data derived from the EMT timecourse predicted that several transcription-factor-binding motifs were important regulators of the EMT expression dynamics, including a motif bound by Tead transcription factors (supplementary material Fig. S1A). This analysis suggested that genes that contain a species-conserved Tead-binding MCAT motif are upregulated during an EMT of NMuMG cells (supplementary material Fig. S1A).

To delineate the regulatory role of Tead transcription factors in the EMT process, we utilized NMuMG cells and Py2T murine breast cancer cells derived from a tumor of MMTV-PyMT transgenic mice (Waldmeier et al., 2012), both of which underwent EMT upon treatment with TGF $\beta$  (Fig. 1A). MTfEcad cells have been established from a mammary tumor of a MMTV-Neu transgenic mouse carrying conditional (floxed) alleles of the E-cadherin gene (*Cdh1*). These cells undergo EMT upon Cre-mediated genetic ablation of the E-cadherin gene (MT $\Delta$ Ecad) (Lehembre et al., 2008) (Fig. 1A).

Gene expression profiling and quantitative RT-PCR revealed that the transcripts of all four Tead family members could be detected in the three model systems before, during and after EMT, and that only Tead2 mRNA levels were upregulated across all model systems analyzed (supplementary material Fig. S1B). Based on the robust and reproducible expression of Tead2, we chose to focus on Tead2 and generated polyclonal antibodies specifically detecting Tead2 (supplementary material Fig. S1C–E). Analysis of endogenous Tead2 expression levels in all three EMT model systems by immunoblotting revealed that Tead2 protein levels increase upon EMT induction (Fig. 1B). EMT-associated increased Tead2 expression was solely observed in

Py2T cells stimulated with TGF $\beta$ , whereas other growth factors like EGF, FGF, HGF, IGF, PDGF or IL-6 were not able to induce Tead2 expression (supplementary material Fig. S1F). Furthermore, small interfering RNA (siRNA)-mediated ablation of Smad4 expression during TGF $\beta$ -induced EMT in NMuMG cells did not affect Tead2 expression levels, suggesting that TGF $\beta$ -induced Tead2 expression is independent of canonical TGF $\beta$  signaling (supplementary material Fig. S1G). Notably, siRNA-mediated ablation of Sox4 expression, a transcription factor known to be a crucial regulator of EMT (Tiwari et al., 2013), revealed that Tead2 expression is strictly dependent on Sox4 activity during TGF $\beta$ -induced EMT in NMuMG and Py2T cells (supplementary material Fig. S1H).

Immunofluorescence analysis showed that low levels of nuclear Tead2 were present in epithelial cells, yet a much stronger nuclear staining could be observed in cells that were in the process of undergoing EMT (Fig. 1C, NMuMG and Py2T) or had undergone EMT (Fig. 1C, MT $\Delta$ Ecad). Immunofluorescence staining of the Tead transcriptional co-activators Yap and Taz revealed that they were distributed throughout the cytoplasm and in the nuclei of epithelial cells, as expected in sparsely growing, proliferating cells (Zhao et al., 2010) (Fig. 1C). Conversely, NMuMG and Py2T cells undergoing TGF $\beta$ -induced EMT or stably mesenchymal MT $\Delta$ Ecad cells displayed predominantly a nuclear localization of Yap and Taz, highly similar to that of Tead2 (Fig. 1C).

We next investigated whether Tead2 binding to Yap and/or Taz was subject to change during an EMT. Co-immunoprecipitation experiments in total cell lysates (Fig. 1D, Py2T, NMuMG) or in cytoplasmic and nuclear cell extracts (supplementary material Fig. S1I) revealed that, indeed, the binding of Yap and Taz to Tead2 increased exclusively in the nucleus upon TGF $\beta$  stimulation. Similarly, both Yap and Taz only bound to Tead2 in mesenchymal MT $\Delta$ Ecad cells and not in epithelial MTfEcad cells (Fig. 1D, MT). From these data we conclude that formation of a nuclear Tead2–Yap–Taz complex is increased during EMT, even though total levels of Yap and Taz decrease upon EMT induction (Fig. 1D; supplementary material Fig. S1I).

Consistent with these observations, we found that pan-Tead transcriptional activity increased upon EMT induction in a Sox4-dependent fashion (supplementary material Fig. S2A–C). Tead transcriptional activity in cells undergoing EMT was assessed by Tead-responsive luciferase reporter constructs bearing either MCAT core motifs (CATTCCT; supplementary material Fig. S2A) (Larkin et al., 1996) or GTTTC core motifs (ACATTCCAC; supplementary material Fig. S2B) (Ota and Sasaki, 2008). In addition, the transcriptional activity of a previously described Cyr61 promoter reporter containing a Tead-responsive MCAT motif (Lai et al., 2011) was induced during EMT of NMuMG cells, whereas mutation of the Tead-binding site resulted in a complete loss of the reporter activity (supplementary material Fig. S2D).

Taken together, these data demonstrate that, upon EMT induction, Tead2 expression levels are increased in a Sox4-dependent manner concomitant with enhanced formation of the Tead2–Yap–Taz complex in the nucleus. In accordance with these observations, overall Tead transcriptional activity increases during EMT.

### Nuclear localization of Yap and Taz is mediated by Tead2 and is required for EMT

From the data presented above, we hypothesized that binding of the increased levels of Tead2 to Yap and Taz in the nucleus is required to activate Tead2-mediated transcriptional activity during EMT. To test this hypothesis, we first investigated whether

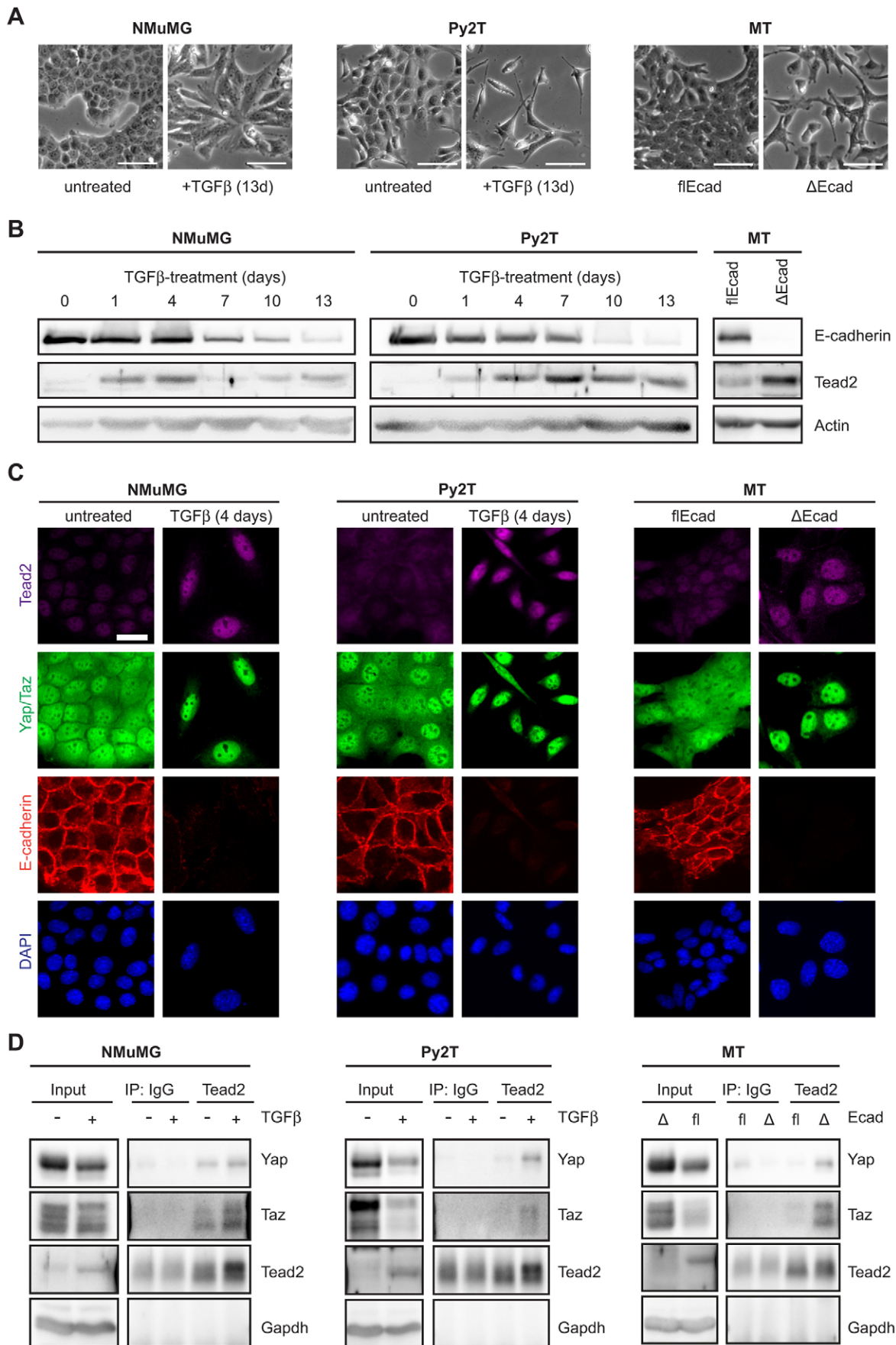


Fig. 1. See next page for legend.

**Fig. 1. Tead2 upregulation and Yap and Taz subcellular redistribution during EMT.** (A) Morphological differences between epithelial and mesenchymal counterparts of the three different cellular EMT model systems used. Epithelial NMuMG and Py2T cells were treated with TGF $\beta$  for 13 days to induce EMT. Stably mesenchymal MT $\Delta$ Ecad cells were derived from epithelial MT $\Delta$ Ecad cells by Cre-recombinase-mediated knockout of the E-cadherin gene. Scale bars: 50  $\mu$ m. (B) Immunoblotting analysis of Tead2 and E-cadherin expression levels before, during and after TGF $\beta$ -induced EMT in NMuMG and Py2T cells, and by genetic deletion in MT $\Delta$ Ecad cells. Actin served as a loading control. (C) Immunofluorescence staining of Tead2 and its co-factors Yap and Taz before and after induction of EMT. Yap and Taz were stained with an antibody that detects both proteins. E-cadherin staining served as a control, DAPI was used to visualize nuclei. Scale bar: 25  $\mu$ m. (D) Interaction of Tead2 with Yap and Taz. Cells were treated with TGF $\beta$  for 4 days (NMuMG) or 7 days (Py2T). Co-immunoprecipitation (IP) was performed with an antibody against Tead2 or irrelevant IgG as a negative control. Levels of Yap, Taz and Tead2 were determined by immunoblotting analysis. Gapdh served as loading control.

overexpression of Tead2 in epithelial cells can provoke a subcellular redistribution of Yap and Taz. Immunofluorescence microscopy analysis revealed that Yap and Taz were evenly distributed between the cytoplasm and nucleus in control cells (Fig. 2A, Vector) or in cells transfected to express a Tead2 mutant (Fig. 2A, Tead2 Y440H), which is incapable of binding to Yap or Taz (Fig. 2A) (Chen et al., 2010; Kitagawa, 2007; Li et al., 2010; Tian et al., 2010; Zhao et al., 2008b). Conversely, the forced expression of wild-type Tead2 (Tead2-WT) in NMuMG cells resulted in a marked concentration of Yap and Taz in the nucleus and reduced levels of cytoplasmic Yap and Taz, suggesting that Tead2 controls Yap and Taz subcellular distribution by direct binding. Consistent with these observations, Tead transcriptional activity was increased by the expression of wild-type Tead2 but not by the expression of mutant Tead2 Y440H (supplementary material Fig. S3A).

We next assessed whether upregulation of Teads during EMT is required for Yap and Taz redistribution and for EMT. NMuMG cells were transfected with control siRNA (siCtr) or with siRNAs against Tead1, 2 and 3 (siTead1-3) whose expression were upregulated during EMT in these cells (supplementary material Fig. S1B). As expected, TGF $\beta$ -treated cells transfected with control siRNA displayed predominantly nuclear localized Yap and Taz in response to TGF $\beta$ -treatment, whereas knockdown of Teads prevented this subcellular redistribution (Fig. 2B). Importantly, depletion of Teads and the resulting failure of Yap and Taz subcellular redistribution also averted the disassembly of tight junctions and adherens junctions normally observed during EMT (supplementary material Fig. S3B). Moreover, immunoblotting analysis of EMT marker expression revealed an attenuation of EMT upon Tead ablation: downregulation of E-cadherin was inhibited and, conversely, upregulation of the mesenchymal markers fibronectin and N-cadherin were delayed (supplementary material Fig. S3C). Similarly, blocking Tead transcriptional activity by the inducible expression of a dominant-negative version of Tead2 (Tead2-EnR) attenuated the EMT process in TGF $\beta$ -treated Py2T cells (supplementary material Fig. S3D,E). These results indicate that Teads are crucial for regulating the cytoplasmic-nuclear redistribution of Yap and Taz during EMT and that this regulatory process is required for EMT.

We next asked whether experimentally increasing Tead2 levels and transcriptional activity in epithelial cells is sufficient to induce EMT. We generated Py2T cells that expressed wild-type Tead2 under the control of the doxycycline-inducible system. Treatment with doxycycline for 3 days led to a heterogeneous

induction of Tead2 expression in these cells (Fig. 2C). Non-induced cells expressing low endogenous levels of Tead2 showed Yap and Taz staining in the cytoplasm as well as in the nucleus. In doxycycline-treated cells, the elevated levels of nuclear Tead2 resulted in concentration of Yap and Taz in the nucleus (Fig. 2C). By 3 days after doxycycline induction, Tead2-expressing cells had already started to lose E-cadherin expression; this phenotype was enforced with a prolonged doxycycline treatment (supplementary material Fig. S3F), indicating that the elevation of Tead2 levels was sufficient to induce EMT.

Yap and Taz nuclear localization, increased formation of Yap–Taz–Tead2 complexes and heightened Tead transcriptional activity was also observed in Py2T cells stably expressing wild-type Tead2 (Tead2-WT) (supplementary material Fig. S3G,H) (Ota and Sasaki, 2008). Notably, although overexpression of a constitutively active version of Tead2 (Tead2-VP16) lacking a Yap- and Taz-binding site showed a transcriptional activity that was highly dependent on Tead (mediated by the *Herpes simplex* virus VP16 transactivation domain), but no increased nuclear localization of Yap and Taz (supplementary material Fig. S3G,I). Furthermore, forced expression of both wild-type Tead2 and constitutively active Tead2-VP16 also resulted in the morphological changes consistent with EMT [i.e. the loss of the epithelial markers E-cadherin and ZO-1, increased expression of the mesenchymal markers vimentin, Zeb1/2 and Slug, and a shift of the cytoskeleton from displaying cortical actin to actin stress fibers (Fig. 2D; supplementary material Fig. S3J)]. Transient siRNA-mediated ablation of Yap or Taz in Tead2-WT (siYap and siTaz, respectively) cells led to a mesenchymal-to-epithelial transition (MET), as indicated by an epithelial morphology and the increased expression of E-cadherin in Yap- or Taz-deficient cells (Fig. 2E,F). Collectively, these results demonstrate that Tead2 is able to induce an EMT via the formation of transcriptionally active complexes with Yap and Taz.

### Tead2 promotes tumor cell migration, invasion and metastasis

A hallmark of cells undergoing EMT is the acquisition of migratory and invasive properties (Nieto, 2011; Yilmaz and Christofori, 2009). Consistent with their mesenchymal phenotype, cells expressing Tead2-WT exhibited an increased capability to migrate and to invade (Fig. 3A). In contrast to control cells, which formed smooth spheres, Tead2-WT and Tead2-VP16 cells invaded three-dimensional Matrigel and projected filopodia into the extracellular matrix (Fig. 3B). These results indicate that, consistent with its EMT-inducing activities, Tead2 also promotes cancer cell migration and invasion.

We next assessed whether Tead2-induced EMT, cell migration and cell invasion translated into a higher metastatic capability in Py2T murine breast cancer cells. Py2T cells stably expressing Tead2-WT, Tead2-VP16 or a control vector were injected into the tail veins of Balb/c nu/nu immune-deficient mice, and the formation of lung metastasis was scored 33 days after injection. Serial sectioning of paraffin-embedded lungs and staining by hematoxylin and eosin revealed that only one out of six mice injected with epithelial control cells displayed macroscopically visible tumor cell clusters. Notably, these nodules were found encapsulated within blood vessels (Fig. 3C,D). In contrast, half of the mice injected with Tead2-WT cells and five out of six mice injected with Tead2-VP16 cells developed macroscopic metastases (Fig. 3C,D), with a higher incidence per mouse as compared to control cells (Fig. 3E).

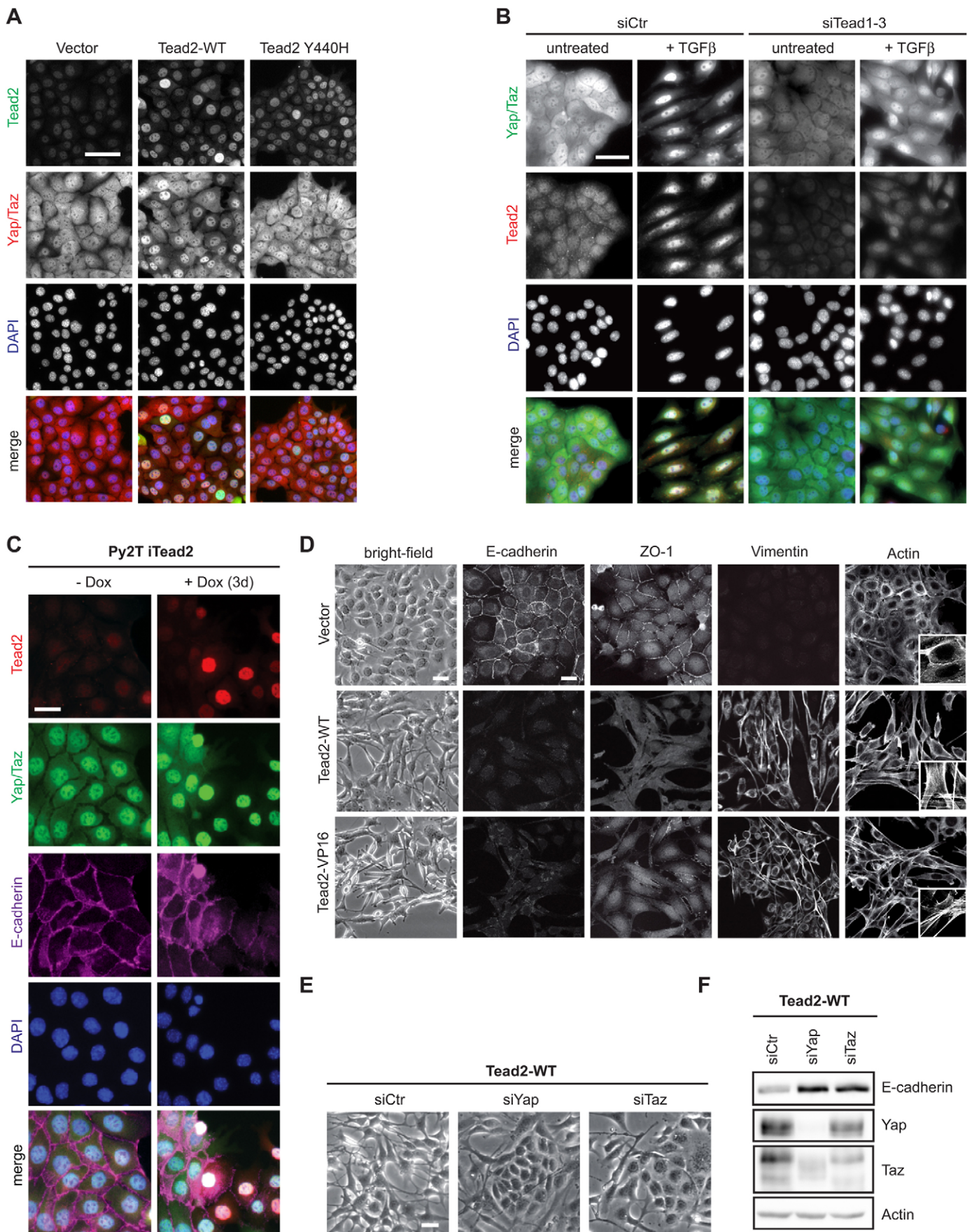


Fig. 2. See next page for legend.

**Fig. 2. Elevated Tead2 levels induce a predominant nuclear localization of Yap and Taz and induce EMT.** (A) Yap and Taz cellular localization is dependent on their direct binding to Tead2. A vector control (Vector), wild-type Tead2 (Tead2-WT) or a Tead2 point mutant defective in Yap and Taz binding (Tead2 Y440H) were stably expressed in NMuMG cells, and Yap and Taz and Tead2 localization was assessed by immunofluorescence staining. DAPI was used to visualize nuclei. Scale bar: 20  $\mu$ m. (B) Depletion of Tead expression prevents the reduction in cytoplasmic levels of Yap and Taz during EMT. NMuMG cells transfected or not with siRNA pools targeting Tead1-3 were induced to undergo EMT by TGF $\beta$ -treatment for 4 days. Yap and Taz, and Tead2 were visualized as described in A. Scale bar: 25  $\mu$ m. (C) Effect of acute Tead2 overexpression on Yap and Taz localization and epithelial differentiation. Tead2 was expressed in Py2T cells (Py2T-iTead2) in a doxycycline (Dox)-inducible fashion, and the localization of Tead2, Yap and Taz and E-cadherin were visualized by an immunofluorescence staining. Scale bar: 20  $\mu$ m. (D) Effect of Tead2 gain-of-function on cell morphology and EMT. Py2T cells were stably transduced with constructs coding for Tead2 (Tead2-WT), a constitutively active version of Tead2 (Tead2-VP16) or an empty vector control. Overall morphological changes were visualized by phase-contrast microscopy and by immunofluorescence staining against E-cadherin, ZO-1, vimentin and the actin cytoskeleton (phalloidin staining). The insets show an enlarged view of F-actin staining. Scale bars: 15  $\mu$ m. (E,F) Depletion of Yap or Taz expression prevents Tead2-induced EMT. Py2T cells stably overexpressing Tead2 were transfected with siRNA pools against Yap and Taz or with a control siRNA (siCtr). Overall cell morphology by phase-contrast microscopy (E) and immunoblotting analysis of E-cadherin, Yap and Taz expression (F) are shown. Scale bar: 15  $\mu$ m.

Taken together, these results indicate that Tead2 promotes increased cancer cell migration/invasion and metastatic outgrowth of Py2T cells in the lung.

### The transcriptional Tead2 target genes during EMT

The results presented above suggest that Tead2 function is regulated differently during EMT, leading to a malignant cancer cell phenotype. To elucidate the corresponding downstream mechanisms we sought to identify genes that are transcriptionally regulated by Tead2 during the process of EMT. Using our Tead2 antibody we performed chromatin immunoprecipitation followed by next generation sequencing (ChIP-Seq) at 5 days of TGF $\beta$ -treatment, a time point at which Tead2 expression and activity was robustly increased in Py2T cells (Fig. 1B; supplementary material Fig. S2A). Detection of known overrepresented transcription factor binding motifs by Hypergeometric Optimization Motif EnRichment (HOMER) revealed that the MCAT Tead-binding motif (supplementary material Fig. S1A) is the most significant motif found in Tead2 bound regions, followed by a motif bound by Jun-AP1 (Fig. 4A). PhyloGibbs, an algorithm that *de novo* infers overrepresented and evolutionarily conserved sequence motifs from ChIP-Seq data,

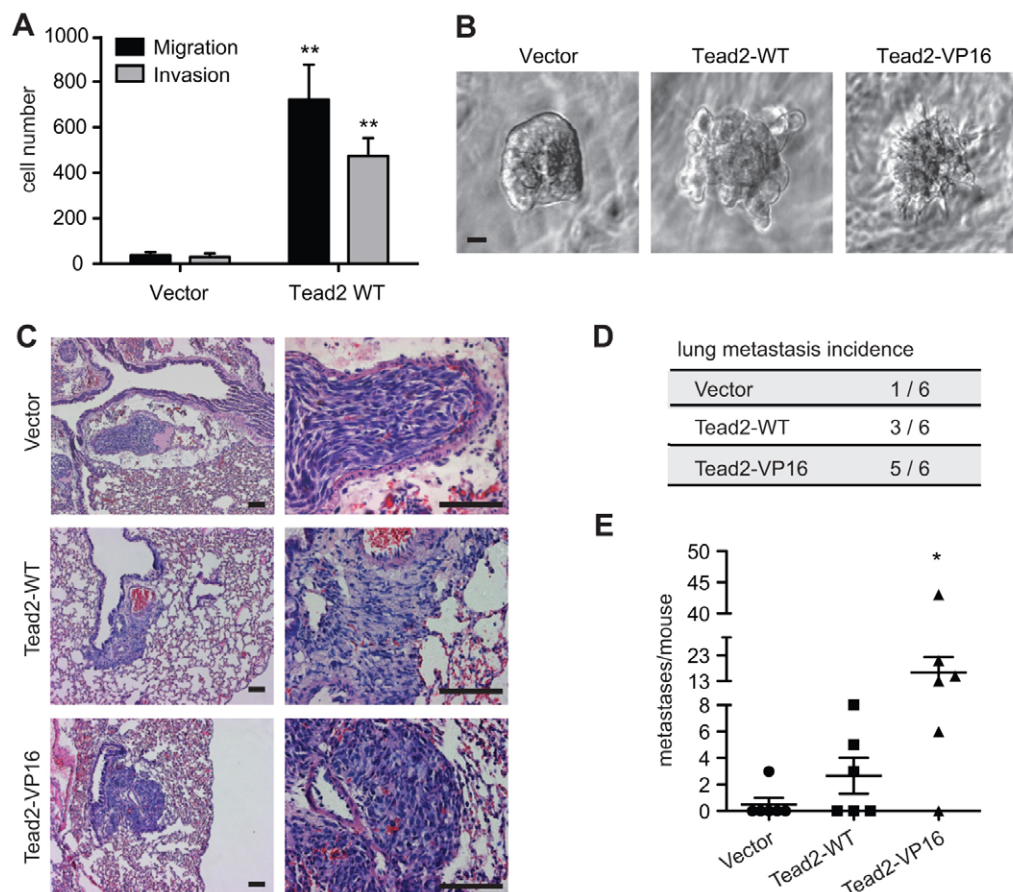


**Fig. 3. Tead2 promotes cell migration, invasion and metastasis.** (A) Chemotactic migration and invasion of Py2T cells stably expressing Tead2-WT or an empty vector control. Transwell assays were performed utilizing cell culture inserts that were not coated (migration) or coated with Matrigel (invasion). Migrated and invaded cells were quantified. Data are shown as mean  $\pm$  s.e.m. ( $n=3$ ; \*\* $P<0.01$ ). (B) Cell invasion in a 3D extracellular matrix. Py2T cells stably expressing Tead2-WT or Tead2-VP16 were embedded in Matrigel and allowed to grow for 5 days. Empty-vector-transduced Py2T cells served as a control. Scale bars: 50  $\mu$ m. (C) Experimental metastasis. Py2T cells as described in B were injected into the tail veins of female Balb/c nu/nu mice. Mice were killed 33 days post-injection and lungs were sectioned and stained by hematoxylin and eosin (H&E). Higher magnifications are also shown (right). Scale bars: 100  $\mu$ m. (D,E) Quantification of lung metastasis incidence and number of lung metastasis per mouse as determined by serial sectioning and microscopic analysis of lungs as described in C. The metastatic incidence was calculated as mice harboring metastases/total number of mice per group. Data are shown as mean  $\pm$  s.e.m. ( $n=6$  mice per group; \* $P<0.05$ ).

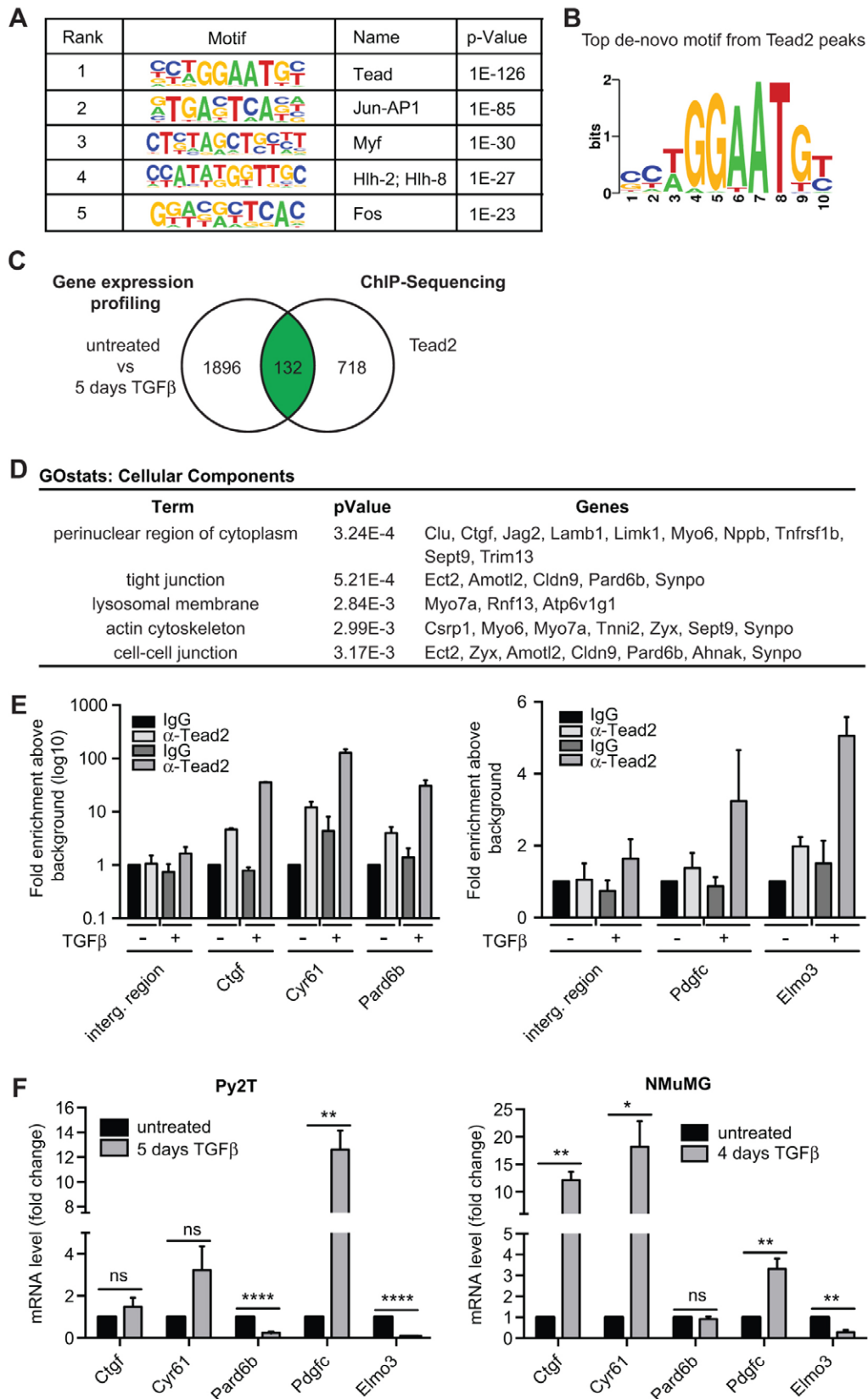


Fig. 4. See next page for legend.

**Fig. 4. Identification of direct Tead2 transcriptional target genes during EMT.** (A) DNA-binding motifs that are overrepresented in Tead2-binding regions. Py2T cells treated with TGF $\beta$  for 5 days were subjected to ChIP using an antibody for Tead2 followed by next generation sequencing (ChIP-Seq;  $n=2$ ). The sequencing data were subjected to Hypergeometric Optimization of Motif Enrichment analysis (HOMER). Shown are the motifs that are significantly enriched. (B) *De novo* generation of sequence motifs overrepresented in Tead2-binding regions using PhyloGibbs. Shown is the most significant Tead2-binding motif. (C) Determination of potential direct target genes of Tead2 during EMT. The Venn diagram depicts the number of genes from the Tead2 ChIP-Seq analysis, the number of genes that were regulated differently in Py2T cells before and after 5 days of TGF $\beta$  treatment and the number of overlapping genes. (D) Gene ontology analysis was performed on overlapping genes described in C using GOstats. The table shows the functional annotation clustering analysis for the top five cellular compartments, the associated genes per group and their  $P$ -values within the groups. (E) Validation of genes directly bound by Tead2 by quantitative PCR. Chromatin from the cells treated as described in A was subjected to qPCR using primer pairs spanning the Tead2-binding regions determined by ChIP-Seq. The data are presented as fold enrichment above background (IP over input) and were normalized to control IgG. An intergenic region was used as negative control. Data are represented as means $\pm$ s.e.m. ( $n=2$ ). (F) Expression of Tead2-bound genes during EMT as determined by RT-qPCR. Py2T and NMuMG cells were treated with TGF $\beta$  for 5 or 4 days, respectively. Fold changes in mRNA expression are presented as means $\pm$ s.e.m. ( $n=3$ ). \* $P<0.05$ , \*\* $P<0.01$ , \*\*\*\* $P<0.0001$ .

also revealed a motif that corresponds to the MCAT and to the highly similar GTIIC core Tead binding motifs (Fig. 4B). These findings suggest that the known MCAT and GTIIC motifs are among the main sequence motifs targeted by Tead2 during TGF $\beta$ -induced EMT.

To identify direct target genes of Tead2 that showed a change in their expression during EMT, we performed genome-wide gene expression profiling in epithelial Py2T cells and in Py2T cells treated with TGF $\beta$  for 5 days. Genes that had a different expression level, passing a cutoff of at least 1.5-fold (adjusted  $P<0.05$ ), were selected for an overlay with Tead2-bound genes as determined by ChIP-Seq analysis (Fig. 4C; supplementary material Table S1). Tead2-bound genes were defined as showing a ChIP-Seq peak at a distance less than 10 kb to their transcriptional start sites (TSS). The overlay analysis identified 132 genes bound by Tead2 in their promoter regions and showing increased or decreased expression during TGF $\beta$ -induced EMT (supplementary material Table S2). Gene ontology analysis for cellular components by GOstats (Ikeda et al., 2009) revealed that Tead2 predominantly controls genes which encode for components of cell junctions and regulators of the actin cytoskeleton (Fig. 4D).

Among these 132 genes, we validated known Tead target genes by ChIP-PCR, including *Ctgf* and *Cyr61* (Zhang et al., 2011), whose expression also increased upon TGF $\beta$ -stimulation in the three EMT model systems investigated (Fig. 4E,F; supplementary material Fig. S4A,B). Furthermore, we identified other candidate Tead2 target genes that had been previously implicated in EMT and/or malignant tumor progression (De Craene and Berx, 2013; Polyak and Weinberg, 2009; Tiwari et al., 2012), such as *Amotl2*, *Esrp2*, *Mal*, *Pdgc*, *Serpine1* and others (supplementary material Table S2). We further ascertained that *Pard6b*, a gene encoding for a polarity complex protein, and *Elmo3*, a gene implicated in phagocytosis and cell migration, were Tead2 target gene candidates. The expression of these genes was decreased during TGF $\beta$ -induced EMT in Py2T and mesenchymal MT $\Delta$ Ecad cells, indicating that Tead2 is not exclusively a transcriptional activator but also a repressor of gene expression (Fig. 4E,F; supplementary material Fig. S4B).

Given that, during EMT, Tead2 formed nuclear complexes with Yap and Taz (Fig. 1D; supplementary material Fig. S11), we assessed whether some of the above-mentioned Tead2-regulated genes were bound by a Tead2–Yap–Taz complex. ChIP experiments for Tead2, Yap and Taz in Py2T cells induced to undergo EMT and subsequent RT-PCR analysis revealed similar or increased binding of Yap and/or Taz to the same promoter regions targeted by Tead2, including the promoters of *Ctgf*, *Cyr61*, *Pard6b*, *Elmo3* and *Pdgc* (supplementary material Fig. S4C).

These results indicate that the Tead2–Yap–Taz complex regulates EMT-relevant genes by acting as a transcriptional activator or repressor, mainly by binding to promoter sequences containing Tead-specific MCAT or GTIIC motifs.

#### Zyxin is a Tead2–Taz target gene critical for EMT

ChIP-Seq also revealed a direct binding of Tead2 to an intronic region of the gene encoding for zyxin (*Zyx*; supplementary material Fig. S4D). Close inspection of this region revealed the presence of a species-conserved MCAT motif (Fig. 5A). Zyxin is an actin regulatory protein that localizes to sites of focal adhesions and stress fibers in response to mechanical cues to facilitate actin polymerization and generation of traction force (Beckerle, 1997; Hirata et al., 2008; Smith et al., 2010). In line with this functional role, zyxin upregulation during EMT in NMuMG cells has been reported to be essential for cell migration (Mori et al., 2009), and given that forced expression of Tead2 promotes cancer cell migration or invasion, and metastatic outgrowth of Py2T cells in the lung (Fig. 4), we decided to focus on zyxin as a Tead2 target gene.

ChIP-PCR on Py2T cells treated with TGF $\beta$  for 5 days confirmed the binding of endogenous Tead2 to an intronic region of the *Zyx* gene (Fig. 5B). Concomitantly, mRNA and protein levels of zyxin were substantially increased during EMT in Py2T cells (Fig. 5C). Higher zyxin expression was also found in mesenchymal MT $\Delta$ Ecad cells as compared to MT $\Delta$ Ecad cells (supplementary material Fig. S4E). Immunofluorescence microscopy analysis confirmed increased levels of zyxin localized along stress fibers that are formed during TGF $\beta$ -induced EMT in Py2T cells and at focal adhesion sites (Fig. 5D), as previously reported (Mori et al., 2009).

To evaluate whether increased expression of zyxin during EMT is dependent on Tead activity, we induced EMT in a pool of Py2T cells expressing a dominant-negative version of Tead2 (Tead2-EnR) under the control of the doxycycline-inducible system. Immunoblotting and RT-PCR analysis demonstrated that expression of Tead2-EnR significantly attenuated zyxin upregulation during EMT (Fig. 5E,F). Similarly, siRNA-mediated knockdown of Tead1, 2 and 3 in NMuMG cells and knockdown of Taz, not Yap, in Py2T cells prevented increased expression of zyxin during EMT (Fig. 5G,H).

We next assessed whether zyxin expression was indeed controlled by Tead2. We thus evaluated zyxin expression in response to modulating Tead2 function by the expression of wild-type Tead2 and Tead2-VP16, by the expression of wild-type Yap and Taz and by the expression of Hippo-signaling-insensitive mutant versions of Yap and Taz (Pan, 2010). Immunoblotting analysis revealed that zyxin expression was induced by forced expression of Tead2-WT, Tead2-VP16 and both versions of Taz, but not by Yap (Fig. 5I,J). These results demonstrate that Tead2 mediates *Zyx* gene expression via Taz co-activation.

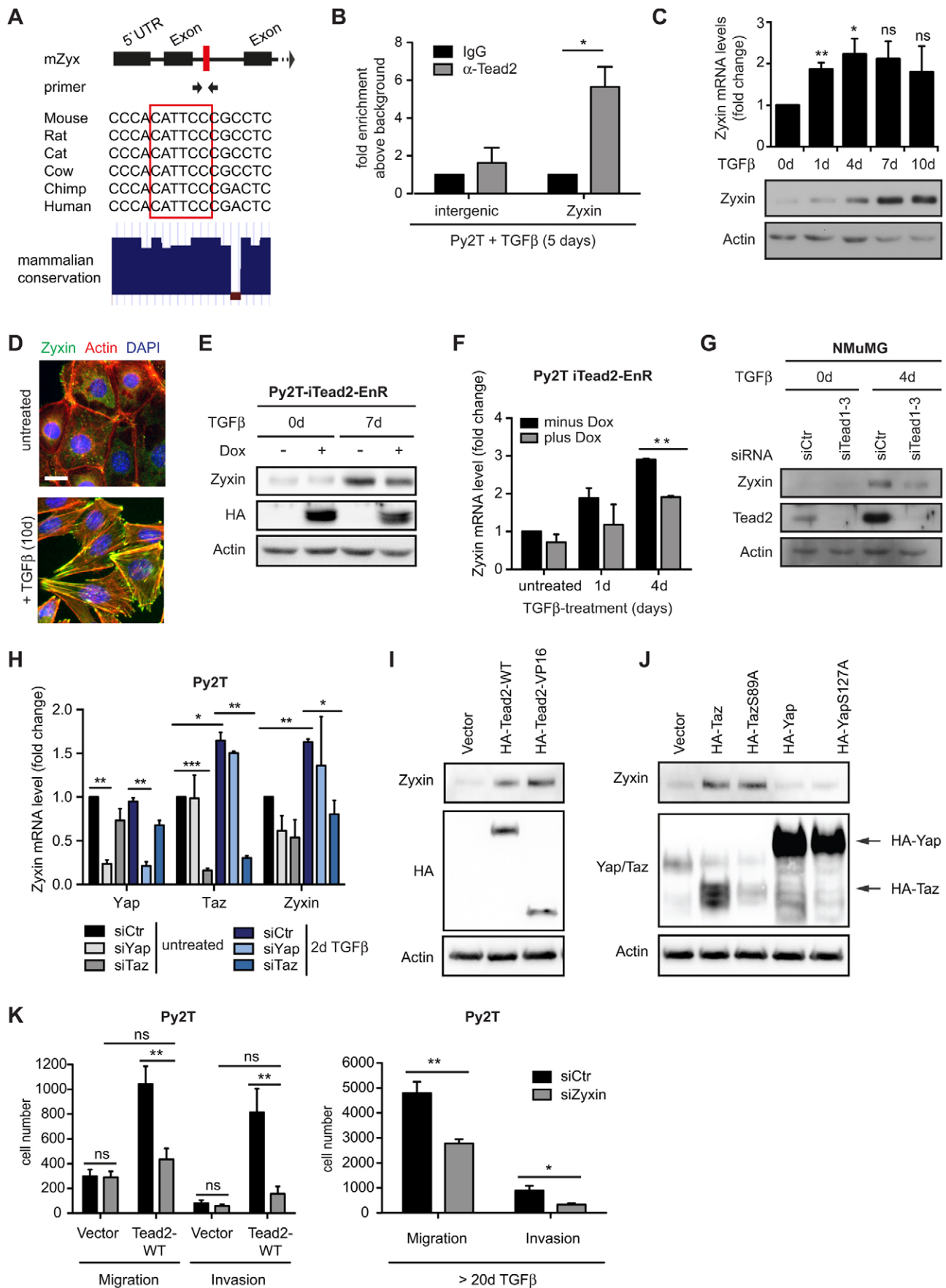


Fig. 5. See next page for legend.

**Fig. 5. Zyxin is a direct Tead2 target gene critical for cell migration.**

(A) Top: scheme of the zyxin gene (*Zyx*) showing the location of the Tead2-binding site (red). Arrows denote primers used in B. Middle: species conservation of the Tead2-binding region. The red box denotes the core MCAT motif. Bottom: mammalian conservation plot encompassing 32 species (derived from UCSC genome browser). (B) Validation of Tead2-binding to the *Zyx* gene by ChIP-qPCR in Py2T cells treated with TGF $\beta$  for 5 days. The qPCR data ( $n=3$ ; mean  $\pm$  s.e.m.; \* $P<0.05$ ) indicate fold enrichment above background and were normalized to irrelevant IgG as negative control. (C) Zyxin expression during EMT. Py2T cells were treated with TGF $\beta$  for the indicated durations. Regulation of mRNA (top) and protein level (bottom) was determined by RT-qPCR and immunoblotting analysis. Results are presented as means  $\pm$  s.e.m. ( $n=3$ ). \* $P<0.05$ ; \*\* $P<0.01$ . (D) Immunofluorescence staining of zyxin and F-actin in epithelial and mesenchymal Py2T cells. Cells were treated with TGF $\beta$  as indicated. F-actin was stained with phalloidin coupled to a fluorophore. Scale bar: 15  $\mu$ m. (E,F) Zyxin protein and mRNA levels in Py2T cells undergoing EMT without (–) or with (+) doxycycline (Dox)-induced expression of a HA-tagged dominant-negative version of Tead2 (Tead2-EnR) before and during a TGF $\beta$ -induced EMT. Results are presented as means  $\pm$  s.e.m. ( $n=2$ ). \*\* $P<0.01$ . (G) Immunoblotting analysis of zyxin during TGF $\beta$ -induced EMT of NMuMG cells transfected with siRNA pools targeting Tead1, 2 and 3 or control siRNA. Membranes shown in supplementary material Fig. S3C were reprobed with an antibody against zyxin. (H) Yap, Taz and zyxin mRNA expression levels in Py2T cells. Cells were transfected with siRNA pools against Yap, Taz or a control siRNA and cultured in the absence and presence of TGF $\beta$ . Results are presented as means  $\pm$  s.e.m. ( $n=2$ ). \* $P<0.05$ , \*\* $P<0.01$ , \*\*\* $P<0.001$ . (I,J) Immunoblotting analysis of zyxin expression in Py2T cells overexpressing HA-tagged wild-type Tead2 (HA-Tead2-WT), constitutively active Tead2 (HA-Tead2-VP16), and wild-type or Yap and Taz mutants (HA-TazS89A, HA-YapS127A). (K) Contribution of zyxin to mesenchymal migration and invasion induced by Tead2 overexpression (Tead2-WT; left panel) or by 20 day TGF $\beta$ -treatment (right panel). Py2T cells were transfected with siRNA pools against zyxin or control siRNA pools and subjected to chemotactic transwell migration and invasion assays as described in Fig. 3A. Data are represented as means  $\pm$  s.e.m. ( $n=3$ ). \* $P<0.05$ , \*\* $P<0.01$ .

To determine the functional contribution of increased zyxin expression levels to cell migration and invasion, we tested whether the increased migratory and invasive phenotype of Py2T cells treated with TGF $\beta$  (>20 days) or of Py2T cells forced to express Tead2-WT (Fig. 3A) could be reversed by siRNA-mediated ablation of zyxin expression (supplementary material Fig. S4G). Indeed, knockdown of zyxin in cells expressing wild-type Tead2 or cells treated with TGF $\beta$  led to a reduction in cell migration and invasion (Fig. 5K). Interestingly, knockdown of zyxin in Py2T cells overexpressing wild-type Tead2 had no effect on the mesenchymal morphology of these cells (supplementary material Fig. S4H), indicating that zyxin is only required for cell migration and invasion and not for the morphogenic process of EMT. The results demonstrate that Tead2 directly regulates zyxin expression during TGF $\beta$ -induced EMT via its co-factor Taz and thereby induces a zyxin-driven migratory and invasive cell phenotype.

**DISCUSSION**

The transdifferentiation of epithelial cells into a mesenchymal state involves a thorough remodeling of cell architecture, such as the loss of apical-basal cell polarity accompanied by a breakdown of tight and adherens junctions. Concomitantly, the establishment of mesenchymal traits involves the generation of front–rear polarity via remodeling of the actin cytoskeleton and the activation of cell migration. These changes largely rely on global changes in gene expression orchestrated by transcription factors (Sánchez-Tilló et al., 2012). Here, we have uncovered a

crucial mechanistic role of Tead transcription factors, in particular Tead2, during the process of EMT.

We demonstrate that Tead2 expression is increased during EMT and that elevated nuclear levels of Tead2 lead to nuclear complex formation with Yap and Taz and to increased nuclear localization of these cofactors. We further demonstrate that increased Tead2 expression during EMT is accompanied by enhanced Tead2-mediated transcriptional activity. Notably, experimental elevation of Tead2 transcriptional activity is sufficient to induce an EMT and the establishment of lung metastasis. The EMT-associated upregulated expression of Tead2 is independent of canonical TGF $\beta$  signaling, because the ablation of Smad4 during TGF $\beta$ -induced EMT had no substantial impact on Tead2 expression. Moreover, our studies indicate that the *Tead2* gene is a downstream target of the transcription factor Sox4, a crucial epigenetic regulator of EMT (Tiwari et al., 2013). Whether *Tead2* gene expression is directly activated by Sox4 during EMT remains to be addressed. Recent studies on SoxC family members, which include Sox4, Sox11 and Sox12, demonstrate a direct regulation of the *Tead2* gene promoter by Sox4 and Sox11 in the fibroblast-like cell line Cos-1 (Bhattaram et al., 2010). Given that Sox4 controls the levels of Tead2, which are crucial for Tead2 binding to the Hippo downstream targets Yap and Taz in nucleus, it will be interesting to assess whether Sox4 is an integrator of non-canonical TGF $\beta$  signaling and Hippo signaling.

Several recent studies have suggested that elevated Tead activity mediated by a gain-of-function of Yap or Taz can evoke a malignant phenotype. Indeed, Taz is highly expressed in ~20% of breast cancers, most of which represent invasive ductal carcinomas (IDCs), and expression of this Tead co-activator is responsible for migration and invasiveness of cultured breast cancer cell lines (Chan et al., 2008). Recently, another study has demonstrated that overexpression of a Hippo-signaling-insensitive version of Yap (YapS127A) renders breast cancer and melanoma cells pro-metastatic (Lamar et al., 2012). In accordance with our results, this effect depends on an intact interaction domain for Yap in Tead, and Tead transcriptional activity correlates with the metastatic potential of various cancer cell lines. Our results are also consistent with previous reports demonstrating that ectopic expression of Yap and Taz in MCF10A normal breast epithelial cells induces EMT via Tead transcriptional activity (Lei et al., 2008; Zhao et al., 2008b).

As expected from cells that have undergone an EMT, we report that Tead2-overexpressing cells display increased migration, invasion and metastasis in comparison to control cells. Conversely, an attenuation of TGF $\beta$ -induced EMT is observed when a dominant-negative version of Tead2 (*Tead2-EnR*) is expressed. This effect is also observed upon siRNA-mediated depletion of Tead family members. These results demonstrate that the presence and transcriptional activity of Teads is required for the proper execution of a TGF $\beta$ -induced EMT program.

Tead transcriptional activity is mainly controlled by the direct binding of the co-factors Yap and Taz (Mahoney et al., 2005; Vassilev et al., 2001; Zhang et al., 2009; Zhao et al., 2008a). Here, we have investigated whether this is also true during EMT in normal mammary epithelial cells and in breast cancer cells. In epithelial cells, Yap and Taz are almost equally distributed between the cytoplasm and the nucleus. However, during EMT Yap and Taz are predominantly localized to the nucleus and this subcellular redistribution is dependent on their binding to Tead2.

We also observe a membranous staining pattern of Yap and Taz in epithelial cells reminiscent of tight junctions (data not shown). This observation is consistent with a series of studies reporting that Yap and Taz clusters with apical junction proteins, such as Crumbs, PATJ, PALS, angiominins and  $\alpha$ -catenin, thereby counteracting their nuclear entry (Chan et al., 2011; Silvis et al., 2011; Varelas et al., 2010a; Varelas et al., 2010b; Wang et al., 2011; Zhao et al., 2011). On the basis of published observations and our own results, it is tempting to speculate that, in epithelial cells, membrane-bound Yap and Taz are released by EMT-induced disassembly of junctional complexes, and increased nuclear levels of a Tead2–Yap–Taz complex in the nucleus to finally promote Tead transcriptional activity.

To the best of our knowledge, this is the first report on genes that are transcriptionally regulated by activated Tead2 during EMT. ChIP-Seq analysis has identified genes that are directly bound by Tead2 during TGF $\beta$ -induced EMT (supplementary material Table S1). Our results indicate that in cells undergoing EMT, Tead2 predominantly binds to regions harboring MCAT Tead-binding motifs (Anbanandam et al., 2006). A closer inspection of Tead2-bound genes and their changes in gene expression during EMT indicates that Tead2 acts as a transcriptional activator as well as a repressor. Because Tead transcription factors lack a transactivation domain, their function depends on transcriptional co-factors. Thus far, Yap and Taz have been reported to exclusively act as transcriptional co-activators of Teads, for example in regulating the expression of the *Ctgf* and *Cyr61* genes (Zhang et al., 2011; Zhao et al., 2008b). Our analysis identified new Tead2 target genes like *Pard6b* and *Elmo3*, whose expression are significantly reduced during EMT. The same promoter regions were also found to be bound by Taz upon TGF $\beta$ -treatment, which would implicate that the Tead2–Taz complex could also function as a transcriptional repressor.

We further report that Taz but not Yap acts as a co-activator of the Tead2 target gene *Zyx*. Zyxin protein expression is upregulated during EMT in a Tead-dependent manner. Zyxin associates with the actin cytoskeleton and therefore can be localized at the apical membrane, in focal adhesions and on stress fibers (Beckerle, 1997). Notably, zyxin is required for the rearrangement of the actin cytoskeleton during TGF $\beta$ -induced EMT of NMuMG cells, thereby enabling cell migration (Mori et al., 2009). Zyxin upregulation could therefore be at least one of the mechanisms by which Tead transcriptional activity controls the induction of a migratory and invasive cellular phenotype during EMT.

In summary, our results establish a crucial regulatory role for Tead transcription factors during the process of EMT and suggest that Teads are not only mere executors of Yap and Taz functions in promoting EMT and metastasis, but also play a crucial regulatory role in controlling Yap and Taz subcellular localization and activity during these processes.

## MATERIALS AND METHODS

### Antibodies and reagents

Antibodies used were as against the following proteins: actin (Santa Cruz Biotechnology, Dallas, TX), E-cadherin (BD, San Jose, CA, USA), N-cadherin (Takara Bio, Otsu, Shiga, Japan), fibronectin (Sigma-Aldrich, St Louis, MO, USA), GAPDH (Sigma-Aldrich), vimentin (Sigma-Aldrich), ZO-1 (Zymed, San Francisco, CA), Yap and Taz (Santa Cruz Biotechnology), Taz (IMGENEX, San Diego, CA, USA), zyxin (Santa Cruz Biotechnology), HA (Covance, Princeton, NJ, USA). Affinity purified, polyclonal rabbit anti-Tead2 antibody was generated by immunizing rabbits with a peptide corresponding to the N-terminus of

Tead2 (amino acids 16–32); phalloidin–Alexa-Fluor-568 was from Invitrogen (Carlsbad, CA). Reagents used were: recombinant human TGF $\beta$ 1 (R&D Systems, Minneapolis, MN, USA); Matrigel, growth factor reduced (BD); Doxycycline (Clontech/Takara).

### Cell culture and cell lines

The subclone of NMuMG cells (NMuMG/E9) was as previously described (Maeda et al., 2005) and was originally obtained from the American Type Culture Collection (ATCC, Manassas, VA). MTfEcad and MT $\Delta$ Ecad cells and Py2T cells are as described previously (Lehembre et al., 2008; Waldmeier et al., 2012). All cells were cultured in Dulbecco's modified Eagle's medium (DMEM) supplemented with glutamine, penicillin, streptomycin and 10% FBS (Sigma-Aldrich). Cells were treated with 2 ng/ml TGF $\beta$ .

### Plasmids

The GTIIC reporter was generated by subcloning the GTIIC Tead response elements including the basal promoter from p $\delta$ 51-LucII (kindly provided by Hiroshi Sasaki, RIKEN Center for Developmental Biology, Kobe, Japan) into pGL4 (Promega, Madison, WI, USA) (Davidson et al., 1988; Ota and Sasaki, 2008). The MCAT reporter was derived from this construct by replacement of 8 $\times$ GTIIC with eight copies of the sequence CCTGACACACATTTCCTCAGCT (8 $\times$ MCAT), where the MCAT core motif is underlined, and flanking sequences were according to Larkin et al. (Larkin et al., 1996). The *Cyr61*prom WT and *Cyr61*prom TeadMut reporters were previously described (Lai et al., 2011) and kindly provided by Xiaolong Yang (Pathology and Molecular Medicine, Queen's University, Ontario, Canada). The *Renilla* luciferase expressing vector (pRL-CMV) was from Promega. Murine Tead1-4 in pcDNA3.1 were kindly provided by Jaime Carvajal (The Institute of Cancer Research, London, UK). Retroviral Tead2-WT and Tead2-VP16 constructs were as described previously (Ota and Sasaki, 2008). Retroviral HA-tagged Tead2, Tead2-VP16, Tead2-EnR, Taz and Yap were created by inserting the respective cDNAs into the pBabe-derived retroviral vector pRFTO containing an N-terminal HA tag (kindly provided by Reto Kohler, FMI, Basel, Switzerland). Original cDNAs were kind gifts from H. Sasaki (Tead2, Tead2-VP16), R. Kohler (Yap, YapS127A) and Kun-Liang Guan (Department of Pharmacology and Moores Cancer Center, UCSD, La Jolla, USA) (Taz, TazS89A). The lentiviral, doxycycline-inducible HA–Tead2 and HA–Tead2-EnR constructs were generated by subcloning from pRFTO into pLVX-tight-puro (Clontech, Madison, WI, USA). Retroviral HA-tagged Tead2 Y440H was generated by PCR-mediated site-specific mutagenesis.

### RNA interference

10 nM siGENOME smart pool siRNAs (Dharmacon, Lafayette, CO, USA) against murine Tead1, Tead2, Tead3, Tead4, Yap, Taz and Zyxin were used for transient knockdown experiments. Transfection was performed with Lipofectamine RNAiMax (Invitrogen) according to the manufacturer's instructions.

### RNA isolation and RT-PCR

Total RNA was prepared using TriReagent (Sigma-Aldrich), reverse transcribed with M-MLV reverse transcriptase (Promega), and transcripts were quantified by PCR using SYBR-green PCR MasterMix (Invitrogen). Riboprotein L19 primers were used for normalization. PCR assays were performed in triplicate, and fold induction was calculated using the comparative Ct method ( $\Delta\Delta$  Ct). Primers used for quantitative RT-PCR are listed in supplementary material Table S3.

### Luciferase reporter assay

Cells were plated in triplicate in 24-well plates. At 1 day after plating, cells were transfected with 800 ng reporter and 10 ng of plasmids encoding *Renilla* luciferase using Lipofectamine 2000 (Invitrogen). Cells were lysed using 1 $\times$  passive lysis buffer (Promega) and lysates were analyzed using the Dual-Luciferase reporter assay system (Promega) and a Berthold Luminometer LB960. Firefly luciferase values were normalized to internal *Renilla* luciferase control values.

### Cell fractionation and co-immunoprecipitation

Nuclear and cytoplasmic extracts were prepared with NE-PER nuclear and cytoplasmic extraction reagents (Thermo Scientific, Waltham, MA, USA) according to the manufacturer's instructions. Protein-G-coupled Dynabeads (Invitrogen) were used for co-immunoprecipitation experiments on total, nuclear and cytoplasmic cell extracts according to the manufacturer's instructions. Samples were analyzed by SDS-PAGE.

### Immunoblotting, immunofluorescence staining, retroviral infection and Affymetrix gene expression profiling

These were performed as described previously (Waldmeier et al., 2012).

### Lentiviral infection

Stable pools of cells expressing Tead2-WT or Tead2-EnR in a doxycycline-inducible fashion were generated using the Lenti-X Tet-On Advanced system (Clontech). Lentiviral particles were produced according to the manufacturer's instructions using the helper vectors pHDM-HGPM2, pHDM-Tat1b, pRC-CMV-RaII and the envelope-encoding vector pVSV. For infection, viral supernatants were added to target cells in the presence of polybrene (8 µg/ml). Cells were spun for 1 hour at 30°C at 1000 g and were subsequently incubated at 37°C under 5% CO<sub>2</sub> in a tissue culture incubator for 2 hours. Viral supernatant was replaced by normal growth medium and after 1 day, antibiotic selection was performed.

### Transwell migration and invasion assay

Trypsinized and washed cells were resuspended in growth medium containing 0.2% FBS and 2 ng/ml TGFβ, where appropriate. 2.5×10<sup>4</sup> cells in 500 µl medium were seeded into cell culture insert chambers (BD). Bottoms of the chambers contained 700 µl of growth medium supplemented with 20% FBS. After 24 hours in a tissue culture incubator at 37°C under 5% CO<sub>2</sub>, cells were fixed with 4% PFA in PBS for 10 minutes. Cells that had not crossed the membrane were removed with a cotton swab, and cells on the bottom of the membrane were stained with DAPI and quantified using a Leica DMI 4000 microscope.

### 3D Matrigel culture

Growth factor-reduced Matrigel (BD) was diluted to 4 mg/ml protein with serum-free growth medium. 2500 cells in 10 µl Matrigel were transferred to one well of a µ-slide angiogenesis microscopy slide (ibidi, Martinsried, Germany). After 20 minutes of gel solidification in a tissue culture incubator, 50 µl of normal growth medium was added. Growth medium was replenished after 3 days. After 5 days of growth, structures were photographed using a Leica DMIL microscope.

### Tail vein injection, tissue processing and H&E staining

0.5×10<sup>6</sup> Py2T cells were injected orthotopically into the tail vein of three months old female Balb/c nude mice. Mice were killed at 33 days post injection and lungs were isolated. Tissue processing and H&E staining were performed as previously described (Waldmeier et al., 2012). All studies involving mice were approved by the Swiss Federal Veterinary Office (SFVO) and the regulations of the Cantonal Veterinary Office of Basel Stadt (licences 1878, 1907, 1908).

### Chromatin immunoprecipitation

ChIP experiments were performed as previously described (Weber et al., 2007). In brief, crosslinked chromatin was sonicated to achieve an average fragment size of 500 bp. Starting with 150 µg of chromatin and 5 µg of antibody, 1/40 of the ChIP sample and a 1:100 dilution of input DNA were used for quantitative PCR per reaction. Fold enrichment of specific target genes was calculated by IP over Input samples and was normalized to IgG negative control. Primers used for ChIP-qPCR are listed in supplementary material Table S4.

### ChIP-Seq

ChIP libraries were prepared using the ChIP-Seq sample Prep Kit from Illumina (San Diego, CA, USA) and were sequenced using Illumina

HiSeq 2000 according to the manufacturer's protocol. ChIP-Seq data were processed as described (Langmead et al., 2009; Stadler et al., 2011). Briefly, reads were mapped against the *Mus musculus* genome (UCSC, mm9) using bowtie software (version 0.9.9.1) with parameters -v 2 -a -m 100, tracking up to hundred best alignment positions per read and allowing at most two mismatches. Each alignment was weighted by the inverse of the number of hits. All quantifications were based on weighted alignments. Chipcor software (<http://sourceforge.net/projects/chip-seq>) was used to estimate the fragment length. Alignments from ChIP-Seq experiments were shifted by half of the estimated fragment length towards their 3' end. Clusters of ChIP-Seq read alignments were identified employing MACS software (v.1.3.7.1) (Zhang et al., 2008) using IP and input samples with following parameters: nomodel, gsize=2700000000, tsize=50, pvalue=1e-5 and shiftsize=(chipcor estimate)/2. Resulting peak candidates were further filtered based on the enrichment over the input chromatin and only peaks with at least 4-fold enrichment were used.

### Motif analysis

For HOMER analysis, motif detection in the vicinity of Tead2-binding sites was carried out using the Hypergeometric Optimization of Motif Enrichment tools (HOMER; v4.1) (Heinz et al., 2010). For PhyloGibbs, *de novo* motif generation was used as described previously (Siddharthan et al., 2005).

### Motif activity response analysis

Microarray raw data (.CEL files) were uploaded to <http://ismara.unibas.ch/fcgi/mara> for analysis.

### Statistical analysis

Statistical analysis and graphs were generated using the GraphPad Prism software (GraphPad Software Inc.). Statistical analyses were performed as indicated in figure legends.

### Accession numbers

Gene expression data of Py2T untreated versus five days TGFβ-treated cells and ChIP-Seq data of Tead2 ChIP during TGFβ-induced EMT in Py2T cells are deposited at Gene Expression Omnibus (GEO accession number: GSE55711).

### Acknowledgements

We thank Hiroshi Sasaki, Kun-Liang Guan, Xiaolong Yang, Jaime Carvajal and Reto Kohler for sharing important reagents. We are grateful to Petra Schmidt, Helena Antoniadis, Isabel Galm, Ursula Schmieder and Roland Jost (Department of Biomedicine, University of Basel, Switzerland).

### Competing interests

The authors declare no competing interests.

### Author contributions

M.D. and L.W. designed and performed the experiments, analyzed the data and wrote the manuscript. R.I. performed the bioinformatical analysis of ChIP-Seq and gene expression profiling. P.B., P.A. and E.v.N. performed the MARA analysis and the initial gene expression profiling analysis. G.C. designed the experiments, analyzed the data and wrote the manuscript.

### Funding

This research has been supported by the Swiss National Science Foundation; the Swiss Initiative for Systems Biology (RTD Cellplasticity), the EU-FP7 framework program [grant number TuMIC 2008-201662]; and the Swiss Cancer League. Deposited in PMC for immediate release.

### Supplementary material

Supplementary material available online at <http://jcs.biologists.org/lookup/suppl/doi:10.1242/jcs.139865/-/DC1>

### References

Acloque, H., Adams, M. S., Fishwick, K., Bronner-Fraser, M. and Nieto, M. A. (2009). Epithelial-mesenchymal transitions: the importance of changing cell state in development and disease. *J. Clin. Invest.* **119**, 1438–1449.

- Anbanandam, A., Albarado, D. C., Nguyen, C. T., Halder, G., Gao, X. and Veeraraghavan, S. (2006). Insights into transcription enhancer factor 1 (TEF-1) activity from the solution structure of the TEA domain. *Proc. Natl. Acad. Sci. USA* **103**, 17225–17230.
- Beckerle, M. C. (1997). Zyxin: zinc fingers at sites of cell adhesion. *Bioessays* **19**, 949–957.
- Bhattaram, P., Penzo-Méndez, A., Sock, E., Colmenares, C., Kaneko, K. J., Vassilev, A., Depamphilis, M. L., Wegner, M. and Lefebvre, V. (2010). Organogenesis relies on SoxC transcription factors for the survival of neural and mesenchymal progenitors. *Nat. Commun.* **1**, 9.
- Chaffer, C. L. and Weinberg, R. A. (2011). A perspective on cancer cell metastasis. *Science* **331**, 1559–1564.
- Chan, S. W., Lim, C. J., Guo, K., Ng, C. P., Lee, I., Hunziker, W., Zeng, Q. and Hong, W. (2008). A role for TAZ in migration, invasion, and tumorigenesis of breast cancer cells. *Cancer Res.* **68**, 2592–2598.
- Chan, S. W., Lim, C. J., Chong, Y. F., Pobbati, A. V., Huang, C. and Hong, W. (2011). Hippo pathway-independent restriction of TAZ and YAP by angiomin. *J. Biol. Chem.* **286**, 7018–7026.
- Chen, L., Chan, S. W., Zhang, X., Walsh, M., Lim, C. J., Hong, W. and Song, H. (2010). Structural basis of YAP recognition by TEAD4 in the hippo pathway. *Genes Dev.* **24**, 290–300.
- Davidson, I., Xiao, J. H., Rosales, R., Staub, A. and Chambon, P. (1988). The HeLa cell protein TEF-1 binds specifically and cooperatively to two SV40 enhancer motifs of unrelated sequence. *Cell* **54**, 931–942.
- De Craene, B. and Berx, G. (2013). Regulatory networks defining EMT during cancer initiation and progression. *Nat. Rev. Cancer* **13**, 97–110.
- Heinz, S., Benner, C., Spann, N., Bertolino, E., Lin, Y. C., Laslo, P., Cheng, J. X., Murre, C., Singh, H. and Glass, C. K. (2010). Simple combinations of lineage-determining transcription factors prime cis-regulatory elements required for macrophage and B cell identities. *Mol. Cell* **38**, 576–589.
- Hirata, H., Tatsumi, H. and Sokabe, M. (2008). Zyxin emerges as a key player in the mechanotransduction at cell adhesive structures. *Commun. Integr. Biol.* **1**, 192–195.
- Hong, W. and Guan, K. L. (2012). The YAP and TAZ transcription co-activators: key downstream effectors of the mammalian Hippo pathway. *Semin. Cell Dev. Biol.* **23**, 785–793.
- Ikedo, Y., Kanda, T., Kosugi, S., Yajima, K., Matsuki, A., Suzuki, T. and Hatakeyama, K. (2009). Gastric cancer surgery for patients with liver cirrhosis. *World J. Gastrointest Surg.* **1**, 49–55.
- Jacquemin, P., Hwang, J. J., Martial, J. A., Dollé, P. and Davidson, I. (1996). A novel family of developmentally regulated mammalian transcription factors containing the TEA/ATTS DNA binding domain. *J. Biol. Chem.* **271**, 21775–21785.
- Kalluri, R. and Weinberg, R. A. (2009). The basics of epithelial-mesenchymal transition. *J. Clin. Invest.* **119**, 1420–1428.
- Kaneko, K. J. and DePamphilis, M. L. (1998). Regulation of gene expression at the beginning of mammalian development and the TEAD family of transcription factors. *Dev. Genet.* **22**, 43–55.
- Kitagawa, M. (2007). A Sveinsson's chorioretinal atrophy-associated missense mutation in mouse Tead1 affects its interaction with the co-factors YAP and TAZ. *Biochem. Biophys. Res. Commun.* **361**, 1022–1026.
- Lai, D., Ho, K. C., Hao, Y. and Yang, X. (2011). Taxol resistance in breast cancer cells is mediated by the hippo pathway component TAZ and its downstream transcriptional targets Cyr61 and CTGF. *Cancer Res.* **71**, 2728–2738.
- Lamar, J. M., Stern, P., Liu, H., Schindler, J. W., Jiang, Z.-G. and Hynes, R. O. (2012). The Hippo pathway target, YAP, promotes metastasis through its TEAD-interaction domain. *Proc. Natl. Acad. Sci. USA* **109**, E2441–E2450.
- Langmead, B., Trapnell, C., Pop, M. and Salzberg, S. L. (2009). Ultrafast and memory-efficient alignment of short DNA sequences to the human genome. *Genome Biol.* **10**, R25.
- Larkin, S. B., Farrance, I. K. and Ordahl, C. P. (1996). Flanking sequences modulate the cell specificity of M-CAT elements. *Mol. Cell. Biol.* **16**, 3742–3755.
- Lehembre, F., Yilmaz, M., Wicki, A., Schomber, T., Strittmatter, K., Ziegler, D., Kren, A., Went, P., Derksen, P. W., Berns, A. et al. (2008). NCAM-induced focal adhesion assembly: a functional switch upon loss of E-cadherin. *EMBO J.* **27**, 2603–2615.
- Lei, Q.-Y., Zhang, H., Zhao, B., Zha, Z.-Y., Bai, F., Pei, X.-H., Zhao, S., Xiong, Y. and Guan, K.-L. (2008). TAZ promotes cell proliferation and epithelial-mesenchymal transition and is inhibited by the hippo pathway. *Mol. Cell. Biol.* **28**, 2426–2436.
- Li, Z., Zhao, B., Wang, P., Chen, F., Dong, Z., Yang, H., Guan, K.-L. and Xu, Y. (2010). Structural insights into the YAP and TEAD complex. *Genes Dev.* **24**, 235–240.
- Maeda, M., Johnson, K. R. and Wheelock, M. J. (2005). Cadherin switching: essential for behavioral but not morphological changes during an epithelium-to-mesenchyme transition. *J. Cell Sci.* **118**, 873–887.
- Magee, J. A., Piskounova, E. and Morrison, S. J. (2012). Cancer stem cells: impact, heterogeneity, and uncertainty. *Cancer Cell* **21**, 283–296.
- Mahoney, W. M., Jr, Hong, J.-H., Yaffe, M. B. and Farrance, I. K. G. (2005). The transcriptional co-activator TAZ interacts differentially with transcriptional enhancer factor-1 (TEF-1) family members. *Biochem. J.* **388**, 217–225.
- Milewski, R. C., Chi, N. C., Li, J., Brown, C., Lu, M. M. and Epstein, J. A. (2004). Identification of minimal enhancer elements sufficient for Pax3 expression in neural crest and implication of Tead2 as a regulator of Pax3. *Development* **131**, 829–837.
- Moreno-Bueno, G., Portillo, F. and Cano, A. (2008). Transcriptional regulation of cell polarity in EMT and cancer. *Oncogene* **27**, 6958–6969.
- Mori, M., Nakagami, H., Koibuchi, N., Miura, K., Takami, Y., Koriyama, H., Hayashi, H., Sabe, H., Mochizuki, N., Morishita, R. et al. (2009). Zyxin mediates actin fiber reorganization in epithelial-mesenchymal transition and contributes to endocardial morphogenesis. *Mol. Biol. Cell* **20**, 3115–3124.
- Nieto, M. A. (2011). The ins and outs of the epithelial to mesenchymal transition in health and disease. *Annu. Rev. Cell Dev. Biol.* **27**, 347–376.
- Ota, M. and Sasaki, H. (2008). Mammalian Tead proteins regulate cell proliferation and contact inhibition as transcriptional mediators of Hippo signaling. *Development* **135**, 4059–4069.
- Pan, D. (2010). The hippo signaling pathway in development and cancer. *Dev. Cell* **19**, 491–505.
- Polyak, K. and Weinberg, R. A. (2009). Transitions between epithelial and mesenchymal states: acquisition of malignant and stem cell traits. *Nat. Rev. Cancer* **9**, 265–273.
- Sánchez-Tilló, E., Liu, Y., de Barrios, O., Siles, L., Fanlo, L., Cuatrecasas, M., Darling, D. S., Dean, D. C., Castells, A. and Postigo, A. (2012). EMT-activating transcription factors in cancer: beyond EMT and tumor invasiveness. *Cell. Mol. Life Sci.* **69**, 3429–3456.
- Sawada, A., Nishizaki, Y., Sato, H., Yada, Y., Nakayama, R., Yamamoto, S., Nishioka, N., Kondoh, H. and Sasaki, H. (2005). Tead proteins activate the Foxa2 enhancer in the node in cooperation with a second factor. *Development* **132**, 4719–4729.
- Sawada, A., Kiyonari, H., Ukita, K., Nishioka, N., Imuta, Y. and Sasaki, H. (2008). Redundant roles of Tead1 and Tead2 in notochord development and the regulation of cell proliferation and survival. *Mol. Cell. Biol.* **28**, 3177–3189.
- Scheel, C. and Weinberg, R. A. (2012). Cancer stem cells and epithelial-mesenchymal transition: concepts and molecular links. *Semin. Cancer Biol.* **22**, 396–403.
- Siddharthan, R., Siggia, E. D. and van Nimwegen, E. (2005). PhyloGibbs: a Gibbs sampling motif finder that incorporates phylogeny. *PLOS Comput. Biol.* **1**, e67.
- Silvis, M. R., Kreger, B. T., Lien, W.-H., Klezovitch, O., Rudakova, G. M., Camargo, F. D., Lantz, D. M., Seykora, J. T. and Vasioukhin, V. (2011).  $\alpha$ -catenin is a tumor suppressor that controls cell accumulation by regulating the localization and activity of the transcriptional coactivator Yap1. *Sci. Signal.* **4**, ra33.
- Smith, M. A., Blankman, E., Gardel, M. L., Luettjohann, L., Waterman, C. M. and Beckerle, M. C. (2010). A zyxin-mediated mechanism for actin stress fiber maintenance and repair. *Dev. Cell* **19**, 365–376.
- Stadler, M. B., Murr, R., Burger, L., Ivanek, R., Lienert, F., Schöler, A., van Nimwegen, E., Wirbelauer, C., Oakeley, E. J., Gaidatzis, D. et al. (2011). DNA-binding factors shape the mouse methylome at distal regulatory regions. *Nature* **480**, 490–495.
- Suzuki, H., Forrest, A. R., van Nimwegen, E., Daub, C. O., Balwier, P. J., Irvine, K. M., Lassmann, T., Ravasi, T., Hasegawa, Y., de Hoon, M. J. et al.; FANTOM Consortium; Riken Omics Science Center (2009). The transcriptional network that controls growth arrest and differentiation in a human myeloid leukemia cell line. *Nat. Genet.* **41**, 553–562.
- Thiery, J. P., Acloque, H., Huang, R. Y. and Nieto, M. A. (2009). Epithelial-mesenchymal transitions in development and disease. *Cell* **139**, 871–890.
- Tian, W., Yu, J., Tomchick, D. R., Pan, D. and Luo, X. (2010). Structural and functional analysis of the YAP-binding domain of human TEAD2. *Proc. Natl. Acad. Sci. USA* **107**, 7293–7298.
- Tiwari, N., Gheldof, A., Tatari, M. and Christofori, G. (2012). EMT as the ultimate survival mechanism of cancer cells. *Semin. Cancer Biol.* **22**, 194–207.
- Tiwari, N., Tiwari, V. K., Waldmeier, L., Balwier, P. J., Arnold, P., Pachkov, M., Meyer-Schaller, N., Schübeler, D., van Nimwegen, E. and Christofori, G. (2013). Sox4 is a master regulator of epithelial-mesenchymal transition by controlling Ezh2 expression and epigenetic reprogramming. *Cancer Cell* **23**, 768–783.
- Varelas, X., Miller, B. W., Sopko, R., Song, S., Gregorieff, A., Fellouse, F. A., Sakuma, R., Pawson, T., Hunziker, W., McNeill, H. et al. (2010a). The Hippo pathway regulates Wnt/beta-catenin signaling. *Dev. Cell* **18**, 579–591.
- Varelas, X., Samavarchi-Tehrani, P., Narimatsu, M., Weiss, A., Cockburn, K., Larsen, B. G., Rossant, J. and Wrana, J. L. (2010b). The Crumbs complex couples cell density sensing to Hippo-dependent control of the TGF- $\beta$ -SMAD pathway. *Dev. Cell* **19**, 831–844.
- Vassilev, A., Kaneko, K. J., Shu, H., Zhao, Y. and DePamphilis, M. L. (2001). TEAD/TEF transcription factors utilize the activation domain of YAP65, a Src/Yes-associated protein localized in the cytoplasm. *Genes Dev.* **15**, 1229–1241.
- Waldmeier, L., Meyer-Schaller, N., Diepenbruck, M. and Christofori, G. (2012). Py2T murine breast cancer cells, a versatile model of TGF $\beta$ -induced EMT in vitro and in vivo. *PLoS ONE* **7**, e48651.
- Wang, W., Huang, J. and Chen, J. (2011). Angiomin-like proteins associate with and negatively regulate YAP1. *J. Biol. Chem.* **286**, 4364–4370.
- Weber, M., Hellmann, I., Stadler, M. B., Ramos, L., Pääbo, S., Rebhan, M. and Schübeler, D. (2007). Distribution, silencing potential and evolutionary impact of promoter DNA methylation in the human genome. *Nat. Genet.* **39**, 457–466.

- Yagi, R., Kohn, M. J., Karavanova, I., Kaneko, K. J., Vullhorst, D., DePamphilis, M. L. and Buonanno, A.** (2007). Transcription factor TEAD4 specifies the trophectoderm lineage at the beginning of mammalian development. *Development* **134**, 3827–3836.
- Yilmaz, M. and Christofori, G.** (2009). EMT, the cytoskeleton, and cancer cell invasion. *Cancer Metastasis Rev.* **28**, 15–33.
- Zhang, Y., Liu, T., Meyer, C. A., Eeckhoute, J., Johnson, D. S., Bernstein, B. E., Nusbaum, C., Myers, R. M., Brown, M., Li, W. et al.** (2008). Model-based analysis of CHIP-Seq (MACS). *Genome Biol.* **9**, R137.
- Zhang, H., Liu, C.-Y., Zha, Z.-Y., Zhao, B., Yao, J., Zhao, S., Xiong, Y., Lei, Q.-Y. and Guan, K.-L.** (2009). TEAD transcription factors mediate the function of TAZ in cell growth and epithelial-mesenchymal transition. *J. Biol. Chem.* **284**, 13355–13362.
- Zhang, H., Pasolli, H. A. and Fuchs, E.** (2011). Yes-associated protein (YAP) transcriptional coactivator functions in balancing growth and differentiation in skin. *Proc. Natl. Acad. Sci. USA* **108**, 2270–2275.
- Zhao, B., Lei, Q.-Y. and Guan, K.-L.** (2008a). The Hippo-YAP pathway: new connections between regulation of organ size and cancer. *Curr. Opin. Cell Biol.* **20**, 638–646.
- Zhao, B., Ye, X., Yu, J., Li, L., Li, W., Li, S., Yu, J., Lin, J. D., Wang, C.-Y., Chinnaiyan, A. M. et al.** (2008b). TEAD mediates YAP-dependent gene induction and growth control. *Genes Dev.* **22**, 1962–1971.
- Zhao, B., Li, L., Lei, Q. and Guan, K.-L.** (2010). The Hippo-YAP pathway in organ size control and tumorigenesis: an updated version. *Genes Dev.* **24**, 862–874.
- Zhao, B., Li, L., Lu, Q., Wang, L. H., Liu, C.-Y., Lei, Q. and Guan, K.-L.** (2011). Angiomotin is a novel Hippo pathway component that inhibits YAP oncoprotein. *Genes Dev.* **25**, 51–63.